JOURNAL OF MATERIALS SCIENCE 32 (1997) 4025–4030

Dry and wet oxidation of an Si_2N_2O–ZrO_2 composite material

M. HEIM, J. CHEN
Department of Inorganic Chemistry, Chalmers University of Technology and University of Göteborg, S-412 96 Göteborg, Sweden

R. POMPE
Swedish Ceramic Institute, Box 5403, S-402 29 Göteborg, Sweden

The oxidation behaviour of a low-cost porous Si_2N_2O–ZrO_2 composite material, produced without the use of a sintering aid, was investigated in dry and humid air and argon, respectively, in the temperature range 800–1470 °C. The extent of internal oxidation in dry air was found to be dependent on the oxidation temperature. The material exhibits excellent oxidation resistance at temperatures $\geqslant$1300 °C. A very thin layer containing zirconium silicate which is formed on the internal pore walls, appears to protect the material against further oxidation. External pore sealing was not observed. Water vapour was found to enhance oxidation significantly. It was also found that a short-term oxidation treatment at high temperature protects the material from further oxidation at lower temperatures. External pore closure did not occur.

1. Introduction

Si_2N_2O–ZrO_2 ceramic composite is a high-temperature structural material. Its low cost and promising properties make it attractive for demanding applications in combustion environments.

Previous investigations [1–5] showed that the high-temperature oxidation resistance of the composite strongly depends on the exposure temperature. At temperatures <1250 °C SiO_2 forms on the Si_2N_2O grains. At temperatures >1250 °C, the composite exhibits considerably improved oxidation resistance. This is ascribed to the formation of a $ZrSiO_4$ phase on the internal and external surfaces. For this reason the material has to be pre-oxidized at high temperatures for a short time to create this protective $ZrSiO_4$ layer.

It is known that the presence of water vapour accelerates the oxidation rates of silicon [6, 7], SiC [8–13] as well as Si_3N_4 [14, 15], and catalyses devitrification of the SiO_2 scale formed by oxidation [16].

In this work, the ceramic composite is examined with respect to its ability to withstand various oxidative treatments and the selective effect of oxidative species in humid atmospheres at high temperatures. In particular, the effect of $O_{2(g)}$ and $H_2O_{(g)}$ has been examined. Because the material batches received were not fully consistent with those used in previous investigations [1–5], measurements in dry conditions were also made to establish a reference level. Different models to explain the observed kinetics are discussed.

2. Experimental procedure

2.1. Material and sample preparation

The material examined in this work is a Si_2N_2O–ZrO_2 composite fabricated by dry processing (NPS technique) from silicon and $ZrSiO_4$ at the Swedish Ceramic Institute [17, 18].

$$ZrSiO_4 + 3Si + 2N_2 \rightarrow 2Si_2N_2O + t\text{-} + m\text{-}ZrO_2 \quad (1)$$

All samples were cut into pieces using a diamond saw to a size of about 3 mm × 7 mm × 8 mm, the surfaces were ground and the samples were ultrasonically cleaned in deionized water, acetone, and ethyl alcohol, respectively, before oxidation. Samples investigated by atomic force microscopy (AFM) were polished to a 4000-grit finish.

2.2. Material characterization

The open porosities of samples were determined by water intrusion and the pore-size distributions were measured by the mercury-intrusion method using a Micromeritics Poresizer 9305 instrument. The specific surface area was determined by the BET method. The pore morphology on a cross-section of as-received material was determined by AFM of the type Rasterscope 400 (DME). Phase analyses of the as-sintered and oxidized materials were carried out by X-ray powder diffractometry (XRD) using a Siemens X-ray diffractometer (D5000).

0022–2461

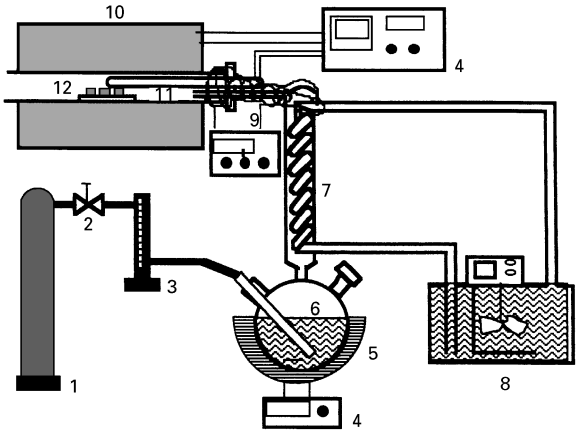

Figure 1 Apparatus for oxidation in humid atmosphere. 1, Gas supply; 2, needle valve; 3, flow meter; 4, temperature controller; 5, mantle heater; 6, evaporator; 7, condenser; 8, thermostat; 9, ribbon heater; 10, electric tube furnace; 11, thermocouple, 12, samples.

2.3. Oxidation

2.3.1. Dry oxidation exposure

The exposures in dry air were performed in an alumina tube furnace with alumina sample holders in the temperature range 800–1450 °C. The gas flow rate was 6 l h^{-1}.

2.3.2. Wet oxidation exposure

Wet oxidation experiments were performed using an alumina tube furnace connected to a steam generator, shown in Fig. 1. The gas was bubbled through boiling deionized water with a flow rate of 25 l h^{-1}. The saturated gas passed through a mantle heater which was connected to a thermostat. The bath temperature in the thermostat was set to be 60.4 °C. The excess water vapour condensed in the mantle heater leaving 20% humidity in the carrier gas. To avoid condensation, all surfaces after the condenser were kept warmer than the dew point using heating wires. The temperature in the furnace was in the range 800–1450 °C.

3. Results

3.1. Material characterization

The composite consists of mainly Si_2N_2O, monoclinic and tetragonal ZrO_2, but also $ZrSiO_4$ and Si_3N_4 were found as minor phases. The open porosity was measured to be 20% $\pm$ 2% with an average pore diameter of 70 nm. The as-received density was determined to be 2.9 g cm^{-3}. The BET specific surface area at room temperature was determined for six samples to be 2.06 $\pm$ 0.03 $m^2\,g^{-1}$. As explained later, the weight-gain data are presented based on the calculated total surface area.

The pore structure covers a large range of pore sizes. Fig. 2 shows an AFM image of a pore in the upper range with a diameter of about 10 μm.

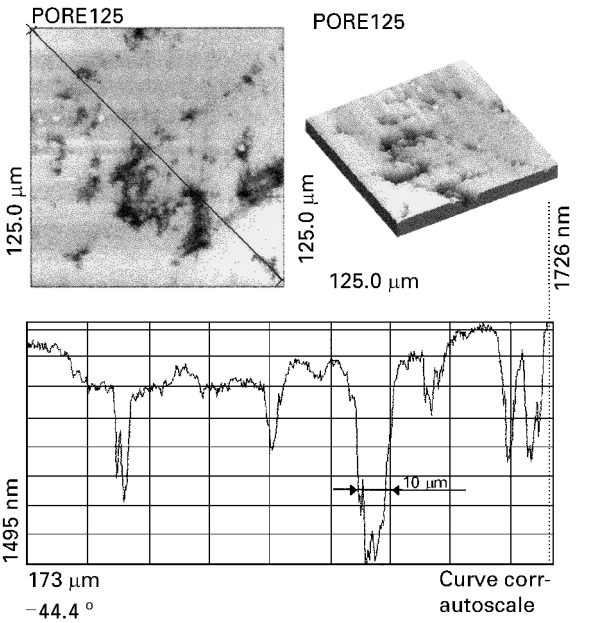

Figure 2 AFM image of polished Si_2N_2O–ZrO_2 (as-received).

3.2. Oxidation

3.2.1. Oxidation in dry air

As can be seen in Fig. 3, at 800 and 1000 °C the weight-gain curves show a parabolic-like growth

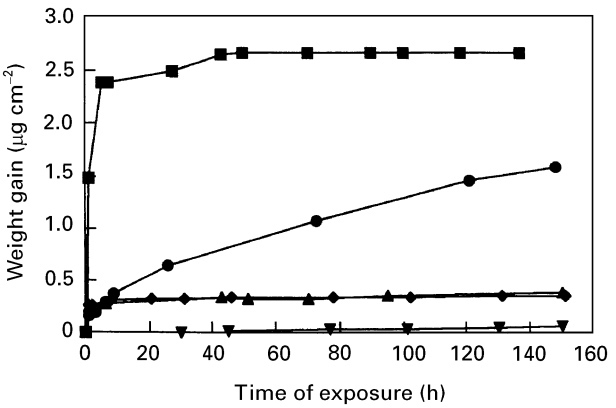

Figure 3 Weight gain of as-received Si_2N_2O–ZrO_2 during oxidation in dry air: (▼) 800 °C, (●) 1000 °C, (■) 1250 °C, (▲) 1350 °C, (◆) 1470 °C.

kinetics and indicate a relatively slow but continuous oxidation of the internal pore surfaces as confirmed earlier [4]. At all other temperatures, rapid weight gains are seen to occur during the first 5 h oxidation, while there is little weight change afterwards. In the temperature range 800–1250 °C, the values of weight gain increase with temperature, while in the range 1250–1470 °C, a considerable drop in the total weight gain occurs. At even higher temperatures (1470 °C), little weight change, as compared to that at 1350 °C, is observed. XRD results show that at temperatures $\leqslant$1250 °C mainly SiO_2 is formed on all surfaces. At higher temperatures, ZrO_2 starts to be involved in the reaction and a relative increase of $ZrSiO_4$ content is detected.

3.2.2. Oxidation in humid atmospheres

Fig. 4 shows the weight gains during oxidation of the as-received material in humid air. During wet oxidation at 800 and 1000 °C the weight gain shows parabolic-like kinetics, but is considerably higher than that

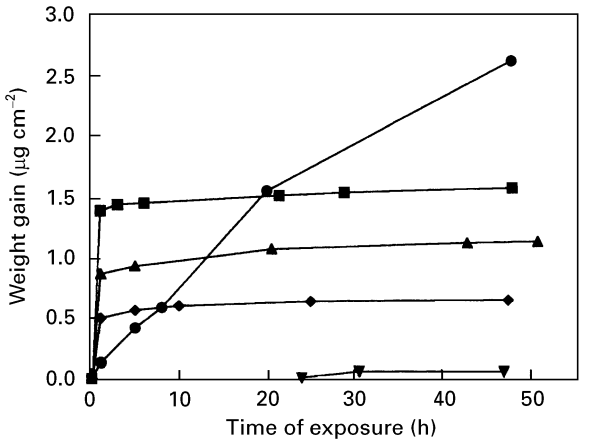

Figure 4 Weight gain of as-received Si_2N_2O–ZrO_2 during oxidation in humid air: (▼) 800 °C, (●) 1000 °C, (■) 1250 °C, (▲) 1350 °C, (◆) 1450 °C.

during dry oxidation. At 1250 °C, samples exposed to dry air show a higher weight gain than those which underwent treatment in humid atmospheres. At temperatures $\geqslant$1250 °C, about 95% of the total weight gain is achieved during the first 5 h oxidation. The weight gain rate then decreases drastically with increasing temperature and zircon starts to appear. At temperatures >1250 °C, wet oxidation kinetics is similar to that in dry oxidation.

3.2.3. Pre-oxidation treatment

In order to investigate the effect of possible pore sealing at the sample surface on the oxidation behaviour, samples were pre-oxidized at 1450 °C for 1 h and further oxidized at 800 and 1250 °C, for 150 h in dry air. A comparison shown in Fig. 5. One can clearly see that after pre-oxidation, the weight becomes stable at 800 °C and the weight gain after pre-oxidation is substantially reduced at 1250 °C compared to that obtained for the as-received material. After pre-oxidation treatment, the phase composition showed the presence of more $ZrSiO_4$ compared to the as-received material and changed little after exposure at lower temperatures.

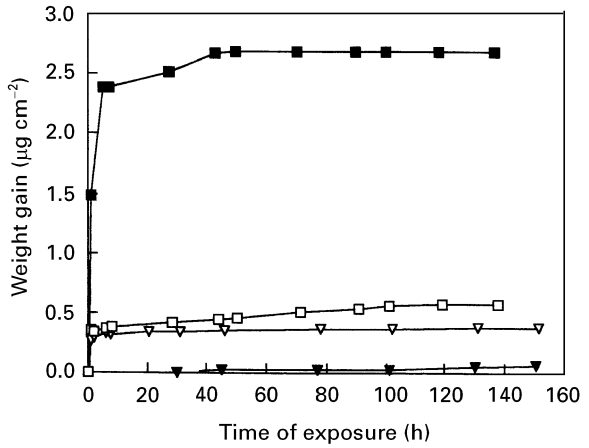

Figure 5 Comparison of oxidation weight gain for the (▼,■) as-received and (▽, □) pre-oxidized Si_2N_2O–ZrO_2 samples at (▼, ▽) 800 °C and (■, □) 1250 °C.

TABLE I Open porosities of oxidized samples before and after surface grinding

Treatment	Open porosity	
	Before grinding (%)	After grinding (%)
As-received; 800 °C, 150 h	17.5	17.1
Pre-oxidized 1450 °C, 1 h; oxidized 800 °C, 150 h	16.4	16.7
As-received; 1250 °C, 150 h	2.9	2.9
Pre-oxidized 1450 °C, 1 h; oxidized 1250 °C, 150 h	15.4	15.8

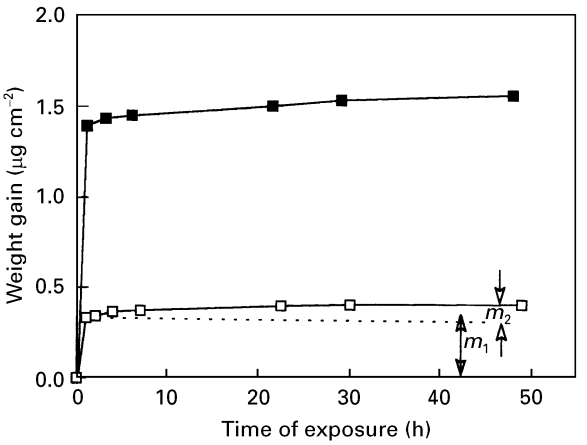

Figure 6 Weight change of (■) as-received and (□) pre-oxidized Si_2N_2O–ZrO_2 during oxidation in humid air at 1250 °C. m_1 = weight gain after the pre-oxidation treatment; m_2 = weight gain after the re-oxidation treatment.

For pre-oxidized samples, the weight gains after re-oxidation treatment were added to the pre-oxidation weight gain. The open porosities of these samples were measured after oxidation and after removing ~500 μm of the sample by grinding on one side of the sample surface. The results are given in Table I.

The open porosities of oxidized samples are seen to remain approximately the same after removal of the surface layer, suggesting that no external pore sealing hand occurred during oxidation.

Fig. 6. shows the results obtained during wet oxidation at 1250 °C of as-received samples and those pre-oxidized in dry air at 1450 °C for 1 h. It can be seen that the pre-oxidation treatment protects the material from oxidation in the presence of water vapour. The weight gain, m_2, for samples after pre-oxidation treatment is much less than that seen for as-received material, and shows an almost zero-weight gain rate.

3.2.4. Effect of partial pressures of oxygen and water

In order to separate the contribution of oxygen and water to oxidation, experiments have been carried out in humid argon, both with as-received and pre-oxidized material. Table II shows the weight gains for all treatments. For samples pre-oxidized at 1450 °C for

TABLE II Weight gains after exposure in different environments

	Weight gain (wt%)				
	800 °C	1000 °C	1250 °C	1350 °C	1450 °C
Dry air, as-received	0.16 (150 h)	3.25 (170 h)	5.50 (140 h)	0.73 (150 h)	0.72 (150 h)
Dry air, pre-oxidized	0.19 (150 h)		0.44 (140 h)		
Wet air, as-received	0.14 (50 h)	5.90 (50 h)	3.00 (50 h)	2.50 (50 h)	1.37 (50 h)
Wet air, pre-oxidized	0.17 (50 h)	0.07 (50 h)	0.19 (50 h)	0.17 (50 h)	0.17 (50 h)
Wet Ar, as-received	0.10 (50 h)	2.40 (55 h)	1.80 (50 h)	1.68 (40 h)	
Wet Ar, pre-oxidized	0.16 (50 h)	0.64 (55 h)	0.18 (50 h)	0.17 (40 h)	

1 h, the weight after pre-oxidation was set to be the origin (cf. m_2 in Fig. 6).

From Table II it can be seen that at 1000 °C, wet oxidation in air (50 h) leads to an oxidation weight gain approximately twice as high as that in dry air (150 h). At 1250 °C (which appears to correspond to a kind of transient oxidation field), the total weight gains become smaller during wet oxidation than those during dry oxidation. This is similar to the observation that, above 1250 °C, any enhanced oxidation will, after a rapid initial stage, lead to a smaller total weight gain, as observed for dry oxidation at $T \geqslant 1250$ °C. At higher temperatures, the total weight gains for wet oxidation are again larger than those during dry oxidation.

Fig. 7 shows the dependence of the final weight gains obtained for samples oxidized at 1350 °C on gas partial pressure, where $p(O_2 + H_2O)$ in a wet argon atmosphere is 20%, in dry air 20.9% and in humid air 36.7%. At comparable partial pressure for samples oxidized in wet argon for 50 h a higher weight gain than in dry air (after 150 h) can be observed.

It has been found that at 800 °C pre-oxidized samples show a higher weight gain than as-received ones. This is thought to be caused by the reaction of the oxidizing species with the Si_2N_2O, forming SiO_2 and then $ZrSiO_4$ during pre-oxidation. The humidity does not cause an increase in weight. At 1000 °C, the protecting effect of the $ZrSiO_4$ layer formed during pre-oxidation treatment becomes dominating. Two effects can be seen: (1) the weight gain levels in wet air are higher than in wet argon, and (2) water vapour appears to enhance oxidation significantly. The pre-oxidized material still show much less weight gain compared to as-received material. At temperatures $\geqslant 1250$ °C the pre-oxidized samples show very low weight gain, and samples exposed to wet argon show less weight gain than those exposed to humid air. This indicates that the zircon-containing protective scale is more efficient against water-vapour attack.

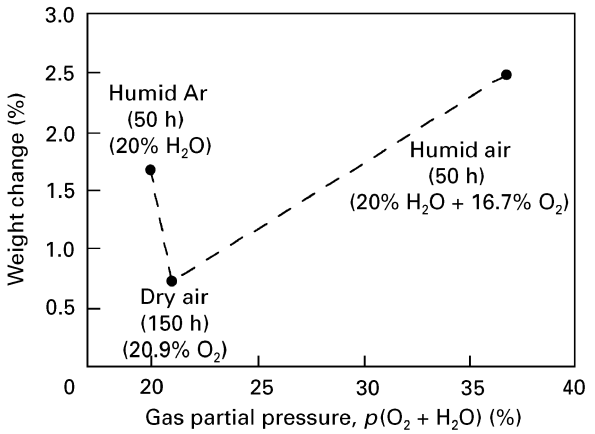

Figure 7 Weight gain as function of gas partial pressure at 1350 °C.

4. Discussion

4.1. Characterization of oxidation kinetics

To describe the oxidation kinetics of a porous nitride ceramics, one may use sample weight change, ΔW, with respect to either the total (internal and external) surface area of the sample ($\Delta W/A_t$), or sample weight ($\Delta W/W$), or external surface area of the sample ($\Delta W/A_{ex}$). $\Delta W/A_t$ (or $\Delta W/W$) may be used when oxidation occurs throughout the sample, as observed during oxidation at relatively low temperatures; $\Delta W/A_{ex}$ may be used if oxidation occurs mainly at the sample's external surface. In a mixed mechanism, however, none of these descriptions is rigorous. It was found that no matter which descriptive method is chosen, the general trend and relative quantity of weight-gain curves remain approximately the same. In this work, $\Delta W/A_t$ has been chosen to plot against oxidation time.

At relatively low temperatures (up to ~1100 °C), the weight-gain curves obey a parabolic law, and oxidation is found to occur at all (internal and external) surfaces [4], which can be expressed by

$$\left(\frac{\Delta W}{A_t}\right)^2 = K_p t \qquad (2)$$

where K_p is the parabolic rate constant which is proportional to the diffusion coefficient and the solubility of the rate-limiting diffusion species in the oxide scale being formed.

At higher temperatures ($\geqslant 1200$ °C), the weight-gain curves appear to be non-parabolic. It may be caused partly, but not completely, by crystallization of the oxidation products being formed [19]. Additional interpretation of the non-parabolic behaviour may be based on further models.

4.1.1. Model I: surface pore closure (previously developed for RBSN) [20]

This model proposes that surface pores seal off in the early stage of oxidation due to the difference in oxygen partial pressure between surface region and internal pore channels. Owing to that difference, the oxide formation in the internal pore channels is hindered by the decreased oxygen partial pressure (due to nitrogen counter-diffusion), more oxide would form near the external surface region than inside the sample. The

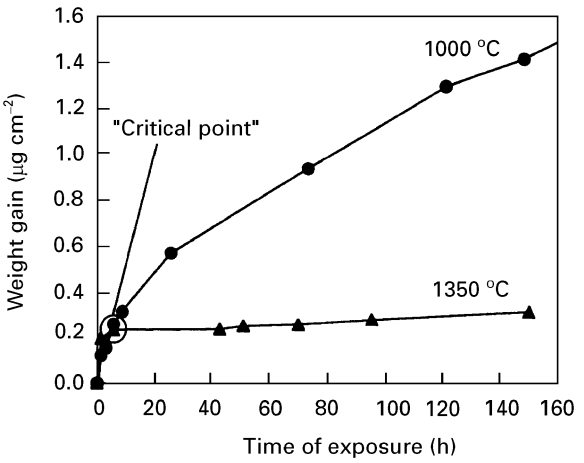

Figure 8 Weight gain of as-received material as function of temperature and time during oxidation in dry air.

surface pore closure would ultimately block further internal oxidation.

This model contradicts the observation that the open porosity remains approximately the same after removal of the surface layer after oxidation (Table I). In addition, the model is not in agreement with the fact that at 1000 °C, the oxidation occurs uniformly in all pore channels, as confirmed by mercury-intrusion [4], without the influence by nitrogen counter-diffusion as described above.

4.1.2. Model II: limited internal pore closure

This proposes that the pores in the sample are interconnected throughout the material. The closure of smaller pore channels may eventually isolate other pore channels or porous areas from oxidant. Once these are blocked, the total accessible surface area decreases significantly, causing the weight gain rate to drop.

This model, however, would not cover the weight-gain behaviour at ~1000 °C, because the curves continue to rise rapidly even beyond "the critical point" (Fig. 8). At this point, the closure of the smaller pore channels would be expected to isolate the large pore areas, this behaviour being consistent with the weight-gain curves at higher temperatures (above 1250 °C).

4.1.3. Model III: zircon as a diffusion barrier

This model assumes that the diffusion coefficient of the rate-limiting diffusion species in zircon is substantially lower than in silica (amorphous + crystalline). When zircon starts to form at higher temperatures (> 1200 °C), it acts as diffusion barrier for the rate-limiting diffusion species, such as O_2, H_2O or N_2.

XRD studies always show that more zircon will be formed at higher temperatures in the temperature range examined. This is consistent with the oxidation rate falling at an earlier stage at a higher temperature. Because zircon may form at all surfaces, a similar level of open porosity of the oxidized sample to that after removal of the surface layer should be expected. This model seems to agree with the present experimental observations.

Based on the collected experimental evidence, a combination of the above-mentioned mechanisms is presumed to be acting at the same time, with predominance of Model III and a contribution of Model II.

The general trend in weight change over the temperature range appears similar to that reported for RBSN materials. However, our previous results [1–5] have shown that the oxidation mechanism for the examined material appears to be rather different from RBSN; i.e. at temperatures $\leqslant$1100 °C, amorphous SiO_2 is formed on surfaces which are accessible to the oxygen, without sealing the pore openings on the external sample surfaces. At higher temperatures, formation of crystallized SiO_2 and $ZrSiO_4$ phases throughout the sample presumably leads to an effective diffusion barrier, protecting the material from further oxidation.

4.2. Effect of water vapour

Separate experiments in a humid atmosphere clearly demonstrate that the values for the weight gain are of the same magnitude when air as the carrier gas is replaced by argon. The effect of water vapour can be readily seen from Fig. 7 where the oxidation weight gain in wet argon is more than twice as much as in dry air. This means that water vapour is the more aggressive oxidant than oxygen. Because high oxidation weight gains are found at higher partial pressures of oxygen and water vapour, the oxidation may be a diffusion-controlled process with oxygen and/or H_2O as the rate-limiting diffusion species. The oxidation reaction may be written

Dry oxidation

$$Si_2N_2O + 3/2O_2 \rightarrow 2SiO_2 + N_2 \quad (3)$$

Wet oxidation (i)

$$Si_2N_2O + 3H_2O \rightarrow 2SiO_2 + 3H_2 + N_2 \quad (4)$$

Wet oxidation (ii)

$$Si_2N_2O + H_2O + O_2 \rightarrow 2SiO_2 + H_2 + N_2 \quad (5)$$

At this point we are not yet able to distinguish the effect of crystallization/devitrification of SiO_2, eventual removal of SiO_2 by evaporation of $Si(OH)_{4(g)}$, and the effect of water vapour on $ZrSiO_4$ formed at higher temperatures. At temperatures above 1200 °C, active oxidation (by $SiO_{(g)}$) can also contribute to the weight change in the Ar/H_2O gas.

5. Conclusions

1. The fall in the weight-gain rate to nearly zero at high temperatures is not caused by surface pore closure.

2. The pre-oxidation treatment at 1450 °C for 1 h in dry air of the Si_2N_2O–ZrO_2 composite significantly improves the oxidation resistance. The effect is presumed to be caused by the formation of a protective diffusion barrier containing zirconium silicate and cristobalite.

3. Water vapour is a more aggressive oxidizing species than oxygen. Water vapour can significantly enhance the oxidation of the Si_2N_2O–ZrO_2 composite in the temperature range 1000–1450 °C.

Acknowledgements

We thank Dr B.-G. Rośen, Department of Production Engineering, Chalmers University of Technology, Sweden, for the AFM measurements. Financial support from the Swedish National Board for Industrial and Technical Development (NUTEK) is gratefully acknowledged.

References

1. M. HEIM, J. CHEN, R. POMPE and H. ARWIN, in "Proceedings of the 5th International Symposium on Ceramic Materials and Components for Engines", edited by D. S. Yan, X. R. Fu and S. X. Shi (World Scientific, Singapore, 1995) pp. 473–76.
2. C. O'MEARA, M. HEIM and R. POMPE, *J. Eur. Ceram. Soc.* **15** (1995) 319.
3. M. HEIM, H. ARWIN, J. CHEN and R. POMPE, *ibid.* **15** (1995) 313.
4. M. HEIM, C. O'MEARA, J. CHEN and R. POMPE, *Ceram. Engng. Sci. Proc.* **17** (4 and 5) (1996) in press.
5. M. HEIM, C. O'MEARA, J. CHEN, R. GATT and R. POMPE, *J. Electrochem.* Soc. in press.
6. E. A. IRENE and R. GHEZ, *J. Electrochem. Soc.* **124** (1977) 1757.
7. B. E. DEAL and A. S. GROVE, *J. Appl. Phys.* **36** (1965) 3770.
8. P. J. JORGENSEN, M. E. WADSWORTH and I. B. CUTLER, *J. Amer. Ceram. Soc.* **44** (1961) 258.
9. J. SCHLICHTING, *Ber. Dt. Keram. Ges.* **56** (1979) 196.
10. *Idem*, *ibid.* **56** (1979) 256.
11. M. MAEDA, K. NAKAMURA and T. OHKUBO, *J. Mater. Sci.* **23** (1988) 3933.
12. E. J. OPILA, *J. Amer. Ceram. Soc.* **77** (1994) 730.
13. E. J. OPILA and R. E. HANN Jr, *J. Amer. Ceram. Soc.*, submitted.
14. S. C. SINGHAL, *ibid.* **59** (1976) 81.
15. M. MAEDA, K. NAKAMURA and T. OHKUBO, *J. Mater. Sci. Lett.* **24** (1989) 2120.
16. P. AINGER, *J. Mater. Sci.* **1** (1966) 1.
17. R. POMPE, US Pat. 438 416, SE Pat. no. 8702268-7 (1987).
18. *Idem*, Patent EPC Co4B 35/48, 35/58 (1988).
19. J. CHEN, M. HEIM and R. POMPE, in "Proceedings of the 4th International Symposium on High Temperature Corrosion and Protection of Materials", May 1996, Les Embiez, France, in press.
20. F. PORZ and F. THÜMMLER. *J. Mater. Sci.* **19** (1994) 1283.

Received 14 June 1996
and accepted 28 January 1997